CLINICAL ORAL IMPLANTS RESEARCH

Jia-Hui Fu
Hector Rios
Khalid Al-Hezaimi
Tae-Ju Oh
Erika Benavides
Hom-Lay Wang

A randomized clinical trial evaluating the efficacy of the sandwich bone augmentation technique in increasing buccal bone thickness during implant placement. II. Tomographic, histologic, immunohistochemical, and RNA analyses

Authors' affiliations:
Jia-Hui Fu, Discipline of Periodontics, Faculty of Dentistry, National University of Singapore, Singapore City, Singapore
Hector Rios, Tae-Ju Oh, Erika Benavides, Hom-Lay Wang, Department of Periodontics and Oral Medicine, School of Dentistry, University of Michigan, Ann Arbor, Michigan, USA
Khalid Al-Hezaimi, Eng A B Growth Factors and Bone Regeneration Research Chair, College of Dentistry, King Saud University, Riyadh, Saudi Arabia

Corresponding author:
Jia-Hui Fu, BDS, MS
11 Lower Kent Ridge Road
Singapore 119083, Singapore
Tel.: +65 6772 4968
Fax: +65 6778 5742
e-mail: denfjh@nus.edu.sg

Key words: biopsy, bone grafts, bone regeneration, dental implants, histology, immunohistochemistry, micro-computed tomography, mRNA

Abstract

Objectives: This study aimed to evaluate the biologic and structural phenotypes of the bone regenerated via the sandwich bone augmentation (SBA) technique, on buccal implant dehiscence defects.

Material and Methods: Twenty-six patients with one buccal implant dehiscence defect each were randomly assigned to two groups. Both groups received a standardized amount of mineralized cancellous and cortical allogenic bone graft. In the test group, a bovine pericardium membrane was placed over the graft, while no membrane was placed in the control group. After 6 months of healing, a bone core biopsy of the regenerated bone was harvested and processed for histologic, immunohistochemical, mRNA, and micro-computed tomography (μCT) analyses. Of the 26 bone core biopsies, only six cores from the test group and six cores from the control group were suitable for the analysis.

Results: Bone volume (BV) in the test group was maintained, but tissue maturation appeared to be delayed. In contrast, tissue maturation appeared to be completed in the control group, but BV was compromised. Micro-CT analysis showed that specimens from the control group were more structured and mineralized compared with those from the test group. Histologic analysis showed more residual graft particles scattered in a loose fibrous connective tissue matrix with sparse bone formation in the test group, while the control group showed obvious vital bone formation surrounding the residual graft particles. Positive periostin (POSTN), sclerostin, *and* runt-related transcription factor-2 (RUNX2) immunoreactivities were detected in both the control and test groups. However, tartrate-resistant acid phosphatase (TRAP) positive was mostly noted in the control group. There were significant differences in *POSTN, RUNX2* and *VEGF* expressions between the test and control groups.

Conclusion: These findings indicated that the SBA technique was an effective method in preserving adequate structural volume while promoting new vital bone formation. Use of the collagen barrier membrane has successfully maintained the volumetric dimensions of the ridge but might have slowed down the complete maturation of the outermost layer of the grafted site.

Date:
Accepted 24 July 2014

To cite this article:
Fu J-H, Rios H, Al-Hezaimi K, Oh T-J, Benavides E, Wang H-L. A randomized clinical trial evaluating the efficacy of the sandwich bone augmentation technique in increasing buccal bone thickness during implant placement. II. Tomographic, histologic, immunohistochemical, and RNA analyses.
Clin. Oral Impl. Res. **26**, 2015, 1150–1157
doi: 10.1111/clr.12481

When a tooth is lost, a well-orchestrated bone remodeling process is activated, leading to horizontal and vertical ridge reduction (Araujo et al. 2005). Unfortunately, this loss of bone is progressive (Pietrokovski & Massler 1967), thus further complicating the rehabilitation of the edentulous ridge over time. As such, surgical techniques and materials are introduced in an attempt to regenerate the lost bone around dental implants so that patients with missing teeth can enjoy improved function, comfort, esthetics, and a better quality of life (Heydecke et al. 2003; Siadat et al. 2008). The first technique was

guided bone regeneration (GBR) (Dahlin et al. 1988), which mimicked the concept of guided tissue regeneration. Following their work, a multitude of surgical techniques, for example, orthodontic extrusion, ridge expansion, sinus floor elevation, distraction osteogenesis, onlay grafts, Le Fort 1 osteotomy, interpositional grafts, and combination of techniques, have been introduced to augment deficient edentulous ridges for implant placement (Pini Prato et al. 2004).

However, as GBR is predictable, easy to use, and relatively less invasive compared to other advanced bone grafting methods (Lee et al. 2009), it is widely used for implant site development (Hammerle et al. 2002; Aghaloo & Moy 2007). This technique utilizes bone grafts and barrier membranes prior to (Buser et al. 1995, 1996) or simultaneously with implant placement (Oh et al. 2003; Wang et al. 2004; Park & Wang 2006; Park et al. 2008; Lee et al. 2009). The sandwich bone augmentation (SBA) technique, which is performed simultaneously with implant placement, has been widely used in recent years (Oh et al. 2003; Wang et al. 2004; Park et al. 2008; Lee et al. 2009). This procedure involves layering of mineralized cancellous and cortical bone allografts to take advantage of the creeping substitution and reverse creeping substitution healing processes of cancellous and cortical bone allografts, respectively (Burchardt 1983). It also mimics the macrostructure of native bone, thereby maximizing the potential of the bone allografts to regenerate bone on exposed implant surfaces (Lee et al. 2009).

Besides the availability of different types of bone grafts, numerous barrier membranes, for example, non-resorbable and absorbable membranes, have been developed to exclude undesirable cells, such as gingival connective tissue cells, from interfering with bone regeneration. Absorbable membranes are preferred because they allow early wound stabilization through faster clot formation, increased migration of fibroblasts to the wound site, increased transfer of nutrients, and ease of handling (Schwarz et al. 2008). Compared to the non-resorbable membranes, a key feature of absorbable membranes is the elimination of a second removal surgery. This greatly decreases possible removal surgery morbidity, chair time, cost, and patient discomfort (Tatakis et al. 1999). A recent clinical trial examined the effect of the bovine pericardium membrane (CopiOs® pericardium membrane; Zimmer Dental Inc., Carlsbad, CA, USA) for guided bone augmentation and found that sites treated with a barrier membrane gained more buccal bone thickness compared to the control sites, which had no barrier membrane (Fu et al. 2014). This is in agreement with others who showed the predictability and efficacy of GBR to augment bone horizontally (Buser et al. 1995; Hammerle et al. 2002; Aghaloo & Moy 2007; McAllister & Haghighat 2007; Park et al. 2008; Jensen & Terheyden 2009). An average ridge width gain of 3.6 mm after a mean healing time of 7.3 months was reported (Jensen & Terheyden 2009), and cumulative implant success or survival rates, respectively, for implants in regenerated bone ranged from 100% after 5 years to 79.4% after 5 years of function (Hammerle et al. 2002).

In terms of implant survival, marginal bone height, and peri-implant soft tissue parameters, implants placed in regenerated bone showed a clinical performance similar to implants placed in native bone (Benic et al. 2009). However, no study has evaluated the quality of this regenerated bone, in terms of tomographic, histologic, immunohistochemical, and mRNA analyses. Certain proteins, representative of bone remodeling and maturation, were thus analyzed. Angiogenesis is critical in the formation of new tissues, for example, bone. Therefore, the presence of vascular endothelial growth factor (VEGF), whose primary function is to stimulate growth of new blood vessels, is important in bone regeneration (Liu & Olsen 2014). Runt-related transcription factor-2 (RUNX2) is a transcription factor that is involved in the differentiation of osteoblasts, rendering it to be an important gene and protein for bone formation (Lian et al. 2004). Periostin, encoded by the *POSTN* gene, is specific to pre-osteoblasts and is a good indicator of a favorable regenerative matrix (Fortunati et al. 2010). Expression of *SOST* gene leads to formation of the protein sclerostin, which is primarily produced by osteocytes. Therefore, it is a good marker for detecting the presence of osteocytes in the regenerated bone (van Bezooijen et al. 2005). Osteoclasts are pivotal in bone remodeling, as bone resorption has to occur prior to bone formation. Tartrate-resistant acid phosphatase (TRAP), expressed by osteoclasts, is thus selected for the analysis (Minkin 1982).

Therefore, this study aimed to examine the structural and biological phenotypes of regenerated bone obtained from the test (bone allografts with pericardium membrane) and control (bone allografts without pericardium membrane) groups. The hypothesis was that a higher degree of mineralization of the regenerated bone and more expression of mRNA and proteins related to angiogenesis, bone formation, and maturation would be associated with the test group compared to the control group.

Material and methods

This randomized, controlled, single masked clinical trial received approval from the University of Michigan Institutional Review Board (Study e-Research ID: HUM00026657) to be conducted from January 15, 2009, to September 19, 2011. Details of the study design could be found in an earlier publication (Fu et al. 2014). Briefly, 26 patients, each with a horizontally deficient edentulous ridge in the maxilla, were recruited into this study, thus achieving a statistical power of 80%. The enrolled patients were randomly assigned to the test and control groups. All sites received a standard narrow or regular platform implant of 3.7 mm or 4.1 mm diameter by 11.5 mm or 13 mm length (Tapered Screw-Vent®; Zimmer Dental Inc.). A buccal implant dehiscence defect was found at all sites, and it was treated with the SBA technique, which used only cancellous and cortical particulate allografts (Puros®; Zimmer Dental Inc.). The test group had a bovine pericardium membrane (CopiOs® pericardium membrane; Zimmer Dental Inc.) placed over the bone grafts, while no membrane was placed in the control group. This bovine pericardium membrane is a three-layer membrane that has a smooth external layer and a fibrillar internal layer. It is made up of non-cross-linked collagen type I bovine pericardial tissue prepared by the Tutoplast® process. As such, this membrane has a three-dimensional fiber structure that possesses the biomechanical stability similar to the extracellular matrix of the connective tissue.

Six months after the implant was placed, a full-thickness mucoperiosteal flap was elevated and a core biopsy of the regenerated bone was taken with a 2.75-mm-diameter trephine positioned perpendicular to the bone surface, away from the implant (Fig. 1). The bone core was divided into two equal sections along its long axis. One section was snap frozen in −80°C liquid nitrogen. The other section was fixed in 10% neutral buffered formalin for 24 h and transferred into 70% ethanol for storage. Particulate cancellous allograft (Puros®; Zimmer Dental Inc., Carlsbad, CA, SUA) and barrier membrane (CopiOs® pericardium membrane; Zimmer Dental Inc.) were placed at the biopsy site. The flaps were approximated and sutured

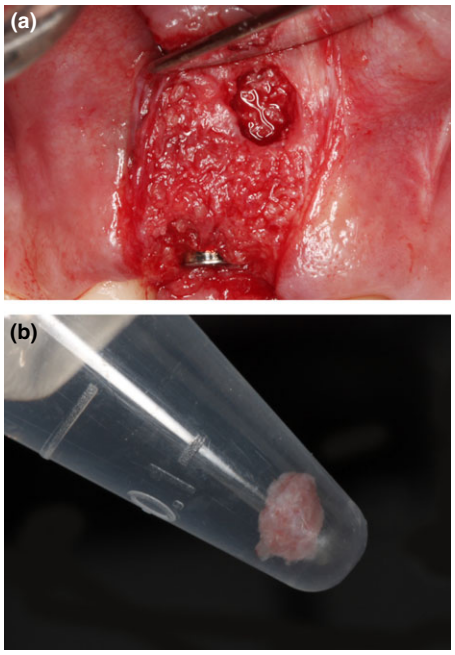

Fig. 1. Clinical site where bone core biopsy was removed from a subject in the test group. (a) Buccal view of regenerated bone and site where bone core biopsy was removed. (b) Thickness of bone core biopsy.

around the healing abutment with 4.0 and 5.0 absorbable sutures (Vicryl®; Ethicon Inc., Sommerville, NJ, USA). The interim prosthesis was adjusted and fitted with no contact at the surgical site. The implant crown was subsequently delivered. Twelve intact bone core biopsies, six from the test group and six from the control group, were obtained.

Micro-computed tomography (μCT) analysis

The bone core biopsy specimens stored in 70% ethanol were placed in a 19-mm-diameter tube and scanned over the entire length of bone using a μCT system (μCT100 Scanco Medical, Bassersdorf, Switzerland) with the scan settings of voxel size 4 μm, medium resolution, 70 kVp, 114 μA, 0.5 mm AL filter, and integration time 500 ms. Analysis was performed using the manufacturer's evaluation software and a set fixed global threshold of 15% (150 on a grayscale of 0–1000) to segment bone from non-bone along the entire length of the bone core. The parameters measured were total volume (TV), bone volume (BV), relative bone volume (BV/TV), trabecular number (Tb.N), trabecular thickness (Tb.Th), trabecular separation (Tb.Sp), apparent density (BMD), and material density (DMB) with results displayed as mean ± standard deviation (SD).

Histologic analysis

The bone core biopsy trephined from the regenerated bone was processed in the Histology Core Facility and Research Laboratory at the University of Michigan, School of Dentistry. The bone specimens were embedded in paraffin, sectioned axially at a thickness of 5 μm, and mounted on microscopic slides (Fisher Superfrost plus; Thermo Fisher Scientific Inc., Waltham, MA, USA). Subsequently, the specimens were stained with hematoxylin and eosin (H&E), dehydrated, paraffinized, and resin mounted.

Immunohistochemical analysis

The specimens were analyzed for the following proteins: TRAP, POSTN, SOST, VEGF and RUNX2. The primary antibody used for detection of TRAP and RUNX2 was a mouse anti-human polyclonal antibody (Abcam®, Cambridge, MA, USA), while the primary antibody used for detection of POSTN, SOST and VEGF was a rabbit anti-human polyclonal antibody (Abcam®). For TRAP and RUNX2 immunolocalization, the optimal primary mouse antibody dilution used was 1 : 75 and 1 : 100, respectively. For POSTN, *SOST* and VEGF immunolocalization, the optimal primary rabbit antibody dilution used was 1 : 8000, 1 : 50, and 1 : 100, respectively.

The specimens were incubated at room temperature with a hydrogen peroxide block (Abcam®) and subsequently washed with a Tris-buffered saline (TBS). They were subjected to an antigen retrieval process using 1% citrate acid buffer and a steam and pressure chamber (Decloaking Chamber™ Plus; Biocare Medical, Concord, CA, USA), following which the specimens were incubated with a protein block (Abcam®) and a blocking kit (Avidin/Biotin blocking kit; Vector Laboratories Inc., Burlingame, CA, USA) was subsequently used to further reduce background stains. The test and control specimens were incubated with the primary antibody and bovine serum albumin in phosphate-buffered saline (BSA/PBS), respectively, at 4°C overnight (>12 h).

The specimens were washed with TBS and incubated with biotinylated IgG (Abcam®) followed by streptavidin peroxidase (Abcam®). They were subsequently treated with a mixture of diaminobenzidine (DAB) chromogen and DAB substrate in a dark environment. The specimens were stained with hematoxylin, dehydrated, paraffinized, and resin mounted.

Specimens for the histologic and immunohistochemical analyses were evaluated under the microscope (Nikon Eclipse 50i, Melville, NY, USA) and photographed using camera software (NIS-Elements D 3.10, Melville, NY, USA).

RNA purification and reverse transcriptase real-time polymerase chain reaction (RT-qPCR) analysis

RNA found in the specimens stored in −80°C was extracted and purified according to the manufacturer's instructions (Trizol® Plus RNA Purification Kit; PureLink™ RNA Mini Kit; Invitrogen Corporation, Carlsbad, CA, USA). The purified mRNA at dilution factor 25 was analyzed for mRNA yield and quality with a spectrophotometer (DU640 Spectrophotometer; Beckman Coulter Inc., Brea, CA, USA). Specimens that did not contain adequate purified mRNA were excluded from the analysis.

The purified mRNA was converted to cDNA (Taqman® RT Reagents kit; Applied Biosystems, Life Technologies Corporation, Carlsbad, CA, USA) after undergoing a reverse transcriptase (RT) reaction in a thermal cycler (MJ Research, GMI, Ramsey, MN, USA). On a 96-well RT-qPCR plate, 8 μl of cDNA (sample) was added to each well, which contained 22 μl of probe and Universal Master Mix (TaqMan® Universal PCR Master Mix; Applied Biosystems, Life Technologies Corporation). The probes used in the qPCR were glyceraldehyde 3-phosphate dehydrogenase (GAPDH) (Assay ID# Hs02758991_g1), POSTN (Assay ID# Hs01566748_m1), RUNX2 (Assay ID# Hs00231692_m1), and VEGF (Assay ID# Hs00900055_m1) (Taqman® probes; Applied Biosystems, Life Technologies Corporation). *GAPDH* served as the housekeeping gene. Each plate contained triplicates of the cDNA templates. The plate was centrifuged to displace the solutions to the base of the well and subsequently sealed tight.

The RT-qPCR process was performed using the 7500 Real Time PCR System (Applied Biosystems, Life Technologies Corporation) under the following condition. For each probe, relative expression of mRNA in the test and control groups was normalized to *GAPDH*. Normalized target gene expression level was calculated using the comparative cycle threshold method known as the $2^{\Delta\Delta Ct}$ method.

Statistical analysis

A nonparametric test, the Mann–Whitney test, in a commercially available statistical package (SPSS® 22.0; IBM Corporation, Armonk, NY, USA) was used to compare the μCT parameters and mean relative mRNA expression between the test and control groups with an α-level = 0.05.

Results

Volumetric data

Over a time period of 6 months, significantly less bone resorption was observed at sites treated with a bovine pericardium membrane (test group) ($P = 0.021$). The test group had approximately 1 and 2 mm more buccal bone gain at 2 and 4 mm apical to the bone crest, respectively (Table 1) (Fu et al. 2014). The clinical measurements indirectly inferred the changes in BV in the test and control groups over the 6-month healing period.

Micro-μCT analysis

No significant differences were found between the test ($n = 6$) and control ($n = 6$) groups (Table 2). There were two structural indices – Tb.N and Tb.Sp, which showed slight differences between the two groups ($P = 0.080$). The test group had greater amount of marrow thickness, thus resulting in a higher Tb.Sp value (test: 0.33 ± 0.03 mm vs. control: 0.24 ± 0.05 mm) ($P = 0.080$), which could be the reason for the comparatively lower BV/TV and BMD values. The control group was found to have greater trabecular number (test: 2.84 ± 0.55 mm^{-1} vs. control: 3.44 ± 0.37 mm^{-1}) ($P = 0.080$), which might have contributed to the higher mineral content of the specimens examined. In general, images taken from the control group appeared to be more consolidated with a structural pattern that resembled bone as compared to the test group, which seemed to be made up of non-integrated bone particles. Fig. 2 illustrated the μCT images of representative specimens obtained from the test and control groups. The findings appeared to imply that regenerated bone from the control group had a greater degree of mineralization and structural organization.

Histologic analysis

Histologic images taken from the test group ($n = 6$) showed more residual bone graft particles scattered in a loose fibrous connective tissue matrix. Sparse bone formation was seen along the sides of a few bone graft particles. Majority of the specimens were composed of a loose fibrous matrix instead of bone. On the contrary, obvious vital bone formation surrounding residual bone graft particles was seen in histologic images taken from the control group ($n = 6$). The presence of osteocytes within lacunae arranged in a lamellar pattern was an indication of bone formation and remodeling. Residual bone graft particles were identified by the presence of empty lacunae. These particles had irregular borders, which might indicate resorption of the particles. A dense connective tissue matrix with blood vessels held the bone together. Fig. 3 shows histologic images of representative specimens obtained from the test and control groups.

Immunohistochemical analysis

In sections taken from the test group, a very dense cellular pre-osteoblastic fibrillar matrix that stained positive for POSTN immunoreactivity was observed (Fig. 4a) compared to the control group (Fig. 4b). This matrix appeared to be very dense with little or no signs of blood vessel infiltration. RUNX2 and SOST immunoreactivities were observed at only one specimen. VEGF and TRAP immunoreactivities were negative. This demonstrated that in the membrane-protected group, bone at the outermost surface of the regenerated buccal bone was immature, thus implying that more time might be needed for bone maturation.

In the control group, obvious osteoclastic activity, as identified by positive TRAP immunoreactivity, was observed. This correlated to signs of resorption of native bone and graft particles (Fig. 5), thus indicating that active bone remodeling was present in the regenerated bone. Positive SOST immunoreactivity showed matured osteocytes in lacunae with projecting canaliculi, thus suggesting that vital bone was formed around the bone graft particles (Fig. 6). Interestingly, the initially empty lacuna in the bone graft particle was filled with osteocytes, therefore suggesting that cell migration might have occurred resulting in colonization of lacunae in bone allograft. A fibrillar matrix, identified by positive POSTN immunoreactivity, was also seen around the bone particles (Fig. 4b). Osteoblasts, identified by positive RUNX2 immunoreactivity, were seen lining the surfaces of bone particles (Fig. 7), denoting active bone formation occurring around the allogenic bone particles. VEGF immunoreactivity was not found, thus implying that angiogenesis was absent in these specimens.

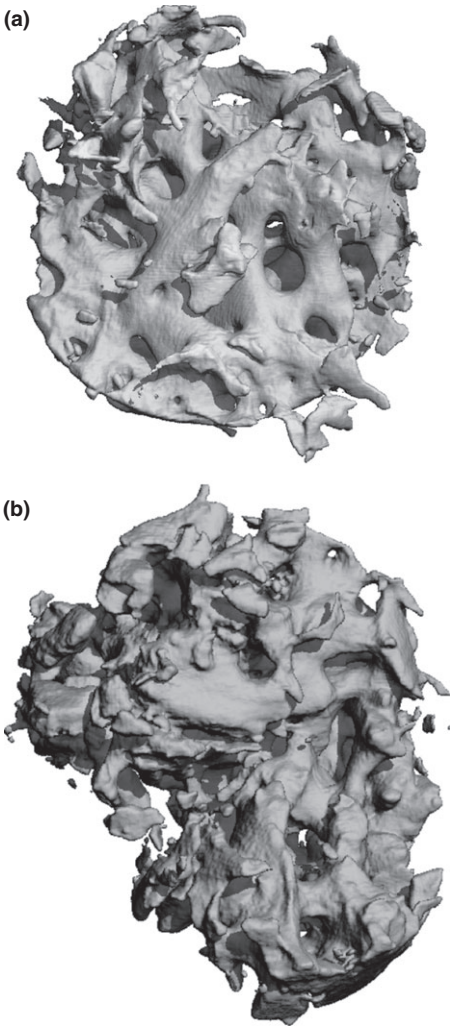

Fig. 2. Micro-computed tomography (CT) image of a representative specimen in the (a) control and (b) test groups.

Table 1. **Summary of the volumetric data (Fu et al. 2014)**

Parameter	Group	Mean ± Standard Error	*P*-value
Horizontal Bone Gain at 2 mm Apical to Crest	Control	0.15 ± 0.262	0.021*
	Test	1.27 ± 0.342	
Horizontal Bone Gain at 4 mm Apical to Crest	Control	0.60 ± 0.431	0.001*
	Test	2.81 ± 0.448	
Horizontal Bone Gain at 6 mm Apical to Crest	Control	0.81 ± 0.485	0.001*
	Test	3.25 ± 0.386	

*Significance at $P < 0.05$.

Relative mRNA expression

Normalizing the relative mRNA expression against the housekeeping gene (*GAPDH*) allowed for comparison between the test and control groups. The $2^{\Delta\Delta Ct}$ method was used to calculate gene expression levels of *POSTN*, *RUNX2* and *VEGF* relative to *GAPDH*. Mean relative *POSTN* expression was greater in the test group (3.21 ± 0.76) compared with the

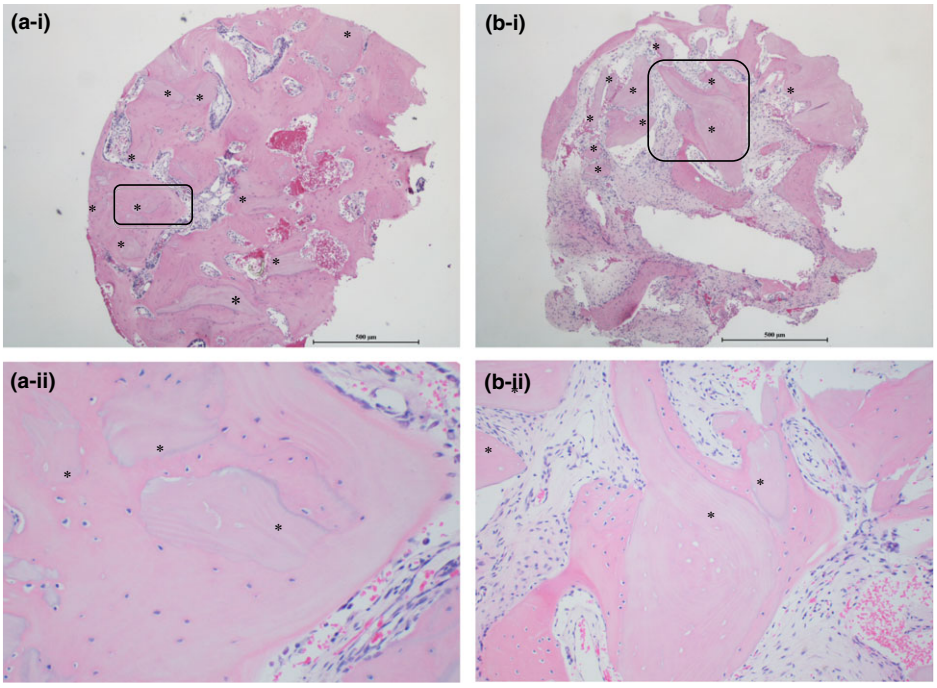

Fig. 3. Histologic images stained by H&E of representative subjects in the (a) control and (b) test groups under magnification (i) 4× and (ii) 10× (box). *Denotes residual allogenic bone graft particles.

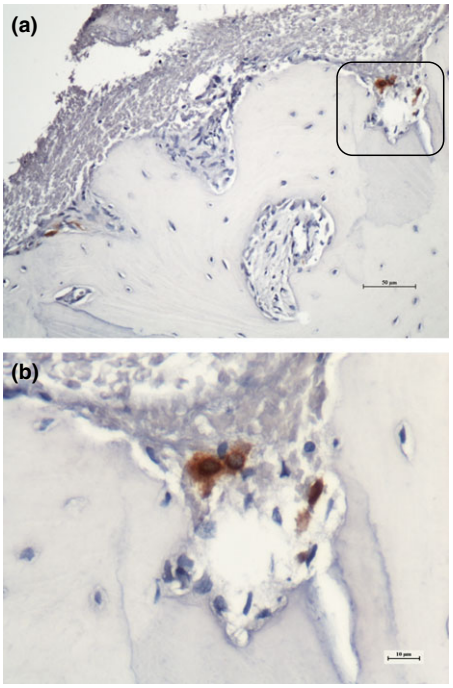

Fig. 5. Histologic images showing positive TRAP immunoreactivity in the control group under magnification (a) 20× and (b) 60× (box).

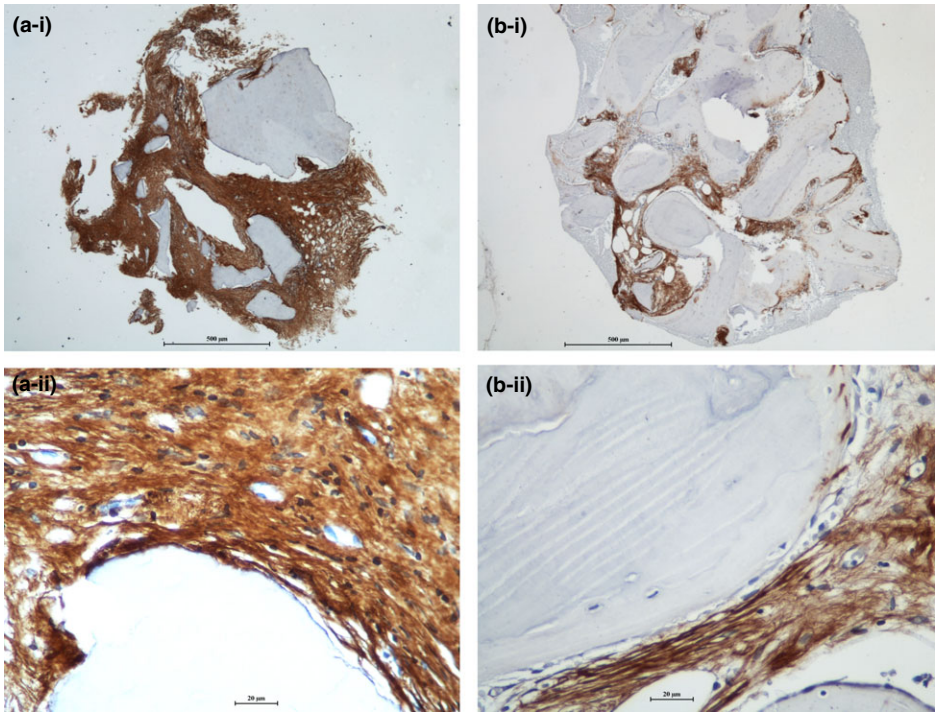

Fig. 4. Histologic images showing positive POSTN immunoreactivity in (a) test and (b) control groups under magnification (i) 4× and (ii) 40×.

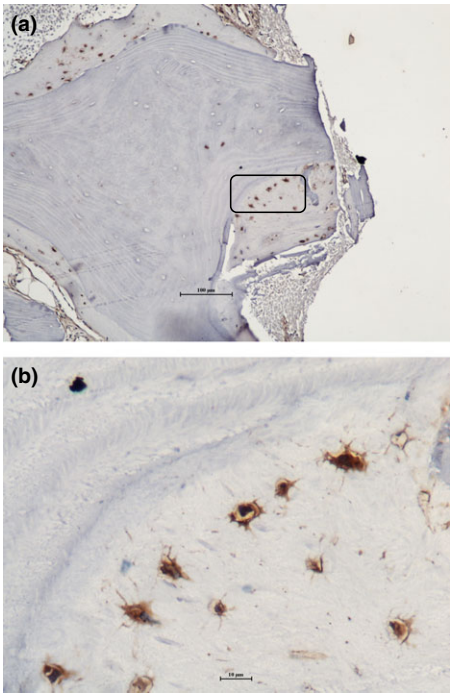

Fig. 6. Histologic images showing positive SOST immunoreactivity in the control group under magnification (a) 10× and (b) 60× (box).

control group (1.07 ± 0.35) (P = 0.080). Mean relative *RUNX2* expression was greater in the control group (1.29 ± 0.45) compared with the test group (1.14 ± 0.27) (P = 0.567). Mean relative *VEGF* expression was greater in the control group (1.80 ± 0.83) compared with the test group (0.73 ± 0.15) (P = 1.000). There were no significant differences in *POSTN*, *RUNX2* and *VEGF* expressions between the test and control groups (Table 2).

Discussion

This study was designed to assess the quality of bone regenerated from mineralized allogen-

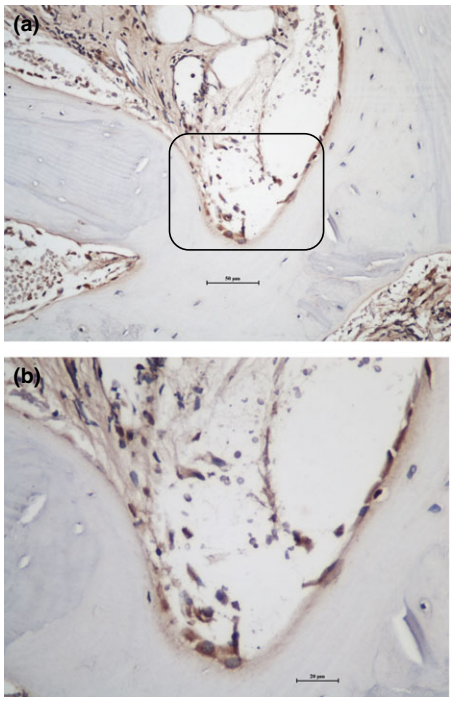

Fig. 7. Histologic images showing positive RUNX2 immunoreactivity in the control group under magnification (a) 20× and (b) 40× (box).

ic particulate bone graft on the buccal or facial surface of dental implants in two experimental groups – in the presence (test group) or absence (control group) of a bovine pericardium membrane, thereby providing the readers with information on the necessity of a barrier membrane and the time needed for healing and maturation of regenerated bone. Clinically, sites in the test group had less bone resorption, better volumetric preservation of the ridge, and thus a greater gain in horizontal bone width at 2, 4, and 6 mm apical to the bone crest.

The μCT analysis showed that the test group had more marrow thickness compared with the control group while the control group had more trabecular number compared with the test group. This implied that specimens from the control group were more mineralized compared with specimens taken from the test group. Specimens from the control group seemed to have a more consolidated structural pattern that resembled bone compared to the test group. The findings appeared to imply that regenerated bone from the control group had a greater degree of mineralization and structural organization. However, there was one limitation associated with this investigation. The μCT analysis could only determine the degree of mineralization of the bone core biopsy harvested and offer a spatial representation of the regenerated bone, but it was unable to differentiate between bone graft particles and mineralized bone. This was because a human mineralized bone allograft that was structurally similar to pristine bone was used (Wang & Tsao 2007).

Therefore, histologic and immunohistochemical analyses were employed to differentiate between vital bone and residual bone allograft. It served to evaluate the biologic phenotype of the regenerated bone by examining the degree of bone maturation and remodeling and the presence and extent of residual bone graft particles. Qualitatively, specimens from the test group generally showed sparse new bone formation around large graft particles surrounded by a fibrous connective tissue matrix, which was a dense pre-osteoblastic fibrillar network rich in POSTN. Periostin is predominantly expressed in fibrous connective tissue such as the periodontal ligament. In bone, it is expressed in the periosteum, but its exact function is still ambiguous. It is, however, speculated to play a role in recruitment of cells of osteoblastic lineage to the regenerative site (Fortunati et al. 2010).

Unlike the test group, specimens from the control group showed obvious vital bone formation surrounding graft particles of irregular sizes and shapes, which was suggestive of osteoclastic resorption of graft particles. Osteocytes within vital mature bone as indicated by the lamellar pattern were also observed. Histologically, the presence of osteocytes and osteoclasts, which indicates bone maturation and remodeling, was identified by positive SOST and TRAP immunoreactivity. Interestingly, migration of osteocytes into the empty lacunae in a human mineralized bone graft particle was seen in a histologic image, thus suggestive of re-inhabitation of the bone graft scaffold by osteocytes instead of osteoclastic resorption of the bone graft particle, followed by new bone formation. This could be attributed to the barrier effect of the periosteum which also served as a source of osteoprogenitor cells and growth factors for bone regeneration (Linde et al. 1993; Jovanovic et al. 1995). In support of the osteogenic or osteopromotive function of the periosteum, a clinical trial showed significant bone regeneration with histologic evidence of vital bone rich in osteoblastic cells in sites regenerated with periosteal coverage (Verdugo et al. 2012).

The RT-qPCR analysis showed expression of mRNA that codes for *POSTN*, *RUNX2* and *VEGF*, which are important for bone formation, maturation, and remodeling. Although RNA levels were detected in the regenerated bone, it was not indicative of protein formation. As such, the immunohistochemical analysis was performed to qualitatively evaluate the presence of proteins related to bone remodeling and maturation, such as TRAP, POSTN, SOST, VEGF and RUNX2.

Analysis of mRNA expression in the representative specimens taken from the test and control groups revealed that *POSTN* expression was markedly elevated. This observation concurred with the recent findings taken from a rat model that investigated relative gene expression of *VEGF*, *POSTN* and *RUNX2* during osseointegration (Lin et al. 2011). During the early healing phase, *POSTN* expression was significantly elevated before arriving at a plateau. In contrast, while *POSTN* expression plateaued, *VEGF* expression decreased and *RUNX2* expression continued to climb. This indicated that active bone formation was occurring as *RUNX2* was the main transcription factor associated with osteoblast differentiation (Komori 2006).

Table 2. **Summary of the micro-computed tomography and relative mRNA expression data**

		Test			Control			
Parameter		Mean	SD	Median	Mean	SD	Median	*P*-value
Micro-CT	TV	9.18	3.78	9.49	5.98	2.66	6.02	0.567
	BV	2.41	0.83	2.45	2.09	1.04	1.57	0.567
	BV/TV	0.28	0.79	0.30	0.36	0.10	0.35	0.567
	Tb.N	2.84	0.55	2.93	3.44	0.41	3.39	0.080
	Tb.Th	0.19	0.02	0.20	0.18	0.03	0.19	1.000
	Tb.Sp	0.33	0.08	0.31	0.24	0.05	0.24	0.080
	BMD	188.59	64.54	212.10	253.96	76.07	240.65	0.180
	DMB	827.05	73.44	820.53	787.41	37.39	801.78	0.567
Mean relative mRNA expression	POSTN	3.21	1.85	2.27	1.07	0.86	0.92	0.080
	RUNX2	1.14	0.66	0.80	1.29	1.09	1.13	0.567
	VEGF	0.73	0.37	0.69	1.80	2.04	0.84	1.000

SD, standard deviation; TV, total volume; BV, bone volume; BV/TV, relative bone volume; Tb.N, trabecular number; Tb.Th, trabecular thickness; Tb.Sp, trabecular separation; BMD, apparent density; DMB, material density; POSTN, periostin; RUNX2, runt-related transcription factor-2; VEGF, vascular endothelial growth factor.

The histologic and immunohistochemical differences observed between the test and control specimens could possibly be due to the bovine pericardium barrier membrane that is made up of non-cross-linked bovine pericardial tissue and has a compact interconnective porous system (Rothamel et al. 2005). It was reported that blood vessel infiltration occurred only 4–8 weeks after implantation and it took 16 weeks for blood vessels to form in the inner layer of the membrane (Schwarz et al. 2006). When the membrane eventually degrades in 4–6 months, osteoprogenitor cells from the periosteum approach the surgical site and contribute to new bone regeneration (Li et al. 2012).

In the test group, the long-lasting pericardium membrane maintained the space for bone regeneration, while in the control group, significant bone resorption occurred (Fu et al. 2014). As a result, the bone biopsies taken from the control group were closer to the implant surface, while those taken from the test group were more superficial. Compared to the test group, there was relatively reduced *POSTN* expression in the control group. Thus, it could be suggested that bone maturation was more complete in areas closer to the implant surface. It could be speculated that in the test group, the outermost layer of the regenerated bone was an immature pre-osteoblastic fibrillar matrix, as indicated by the marked *POSTN* expression. Once again, it was suggestive that more time might be needed for complete bone maturation in the membrane-treated sites.

The size of the bone core biopsy was a major limiting factor in the analysis. On average, the bone core biopsy obtained was 2.71 mm diameter by 1.34 mm thick. This specimen was taken from the buccal surface of the regenerated bone and further divided into two portions for the separate analyses. Because the specimen was taken rather superficially, a high possibility exists that the top surface of the regenerated bone has more fibrous tissue infiltration compared with the deeper sections. In addition, simply because of the sheer size of the biopsy, there is a high possibility that essential cells are not detected. It was also technically difficult to extract sufficient amounts of purified RNA for RT-PCR analysis. As such, valuable information might have gone undetected.

As the total thickness of regenerated bone on the buccal or facial surface of implants in the test group was not completely matured prior to functional loading, the behavior of this bone under functional loading over time needs further validation.

Conclusion

Although the bone thickness was maintained in sites that had a barrier membrane, the outermost surface of the regenerated bone was less mineralized and more fibrous, therefore suggesting that a longer healing time was needed for complete maturation of the regenerated bone. In addition, this study provided insight into the bone maturation and remodeling process around a dental implant as demonstrated by the elevation of relative mRNA expression of *POSTN* and the presence of bone mineralization-related proteins such as TRAP, RUNX2, POSTN and SOST.

Acknowledgements: The authors would like to acknowledge Drs. Juan Rodriguez, Miguel Padial, and Sarah Volk from the Department of Periodontics and Oral Medicine, School of Dentistry, University of Michigan, Ann Arbor, for their guidance in the laboratory analysis. This paper was partially supported by Zimmer Dental Inc., Delta Dental Foundation Dental Master's Thesis Award, American Academy of Implant Dentistry Student Research Grant, The R.W. Bunting Periodontal Study Club Research Grant, Rackham Graduate Student Research Grant, and the University of Michigan Periodontal Graduate Student Research Fund. The authors do not have any financial interests, either directly or indirectly, in the products or information listed in the paper.

References

Aghaloo, T.L. & Moy, P.K. (2007) Which hard tissue augmentation techniques are the most successful in furnishing bony support for implant placement? *International Journal of Oral and Maxillofacial Implants* **22**(Suppl): 49–70.

Araujo, M.G., Sukekava, F., Wennstrom, J.L. & Lindhe, J. (2005) Ridge alterations following implant placement in fresh extraction sockets: an experimental study in the dog. *Journal of Clinical Periodontology* **32**: 645–652.

Benic, G.I., Jung, R.E., Siegenthaler, D.W. & Hammerle, C.H. (2009) Clinical and radiographic comparison of implants in regenerated or native bone: 5-year results. *Clinical Oral Implants Research* **20**: 507–513.

van Bezooijen, R.L., ten Dijke, P., Papapoulos, S.E. & Lowik, C.W. (2005) Sost/sclerostin, an osteocyte-derived negative regulator of bone formation. *Cytokine & Growth Factor Reviews* **16**: 319–327.

Burchardt, H. (1983) The biology of bone graft repair. *Clinical Orthopaedics and Related Research* **174**: 28–42.

Buser, D., Dula, K., Belser, U.C., Hirt, H.P. & Berthold, H. (1995) Localized ridge augmentation using guided bone regeneration. II. Surgical procedure in the mandible. *The International Journal of Periodontics & Restorative Dentistry* **15**: 10–29.

Buser, D., Dula, K., Hirt, H.P. & Schenk, R.K. (1996) Lateral ridge augmentation using autografts and barrier membranes: a clinical study with 40 partially edentulous patients. *Journal of Oral and Maxillofacial Surgery* **54**: 420–432; discussion 432–423.

Dahlin, C., Linde, A., Gottlow, J. & Nyman, S. (1988) Healing of bone defects by guided tissue regeneration. *Plastic and Reconstructive Surgery* **81**: 672–676.

Fortunati, D., Reppe, S., Fjeldheim, A.K., Nielsen, M., Gautvik, V.T. & Gautvik, K.M. (2010) Periostin is a collagen associated bone matrix protein regulated by parathyroid hormone. *Matrix Biology* **29**: 594–601.

Fu, J.H., Oh, T.J., Benavides, E., Rudek, I. & Wang, H.L. (2014) A randomized clinical trial evaluating the efficacy of the sandwich bone augmentation technique in increasing buccal bone thickness during implant placement surgery: I. Clinical and radiographic parameters. *Clinical Oral Implants Research* **25**: 458–467.

Hammerle, C.H., Jung, R.E. & Feloutzis, A. (2002) A systematic review of the survival of implants in bone sites augmented with barrier membranes (guided bone regeneration) in partially edentulous patients. *Journal of Clinical Periodontology* **29**(Suppl 3): 226–231; discussion 232–223.

Heydecke, G., Locker, D., Awad, M.A., Lund, J.P. & Feine, J.S. (2003) Oral and general health-related quality of life with conventional and implant dentures. *Community Dentistry and Oral Epidemiology* **31**: 161–168.

Jensen, S.S. & Terheyden, H. (2009) Bone augmentation procedures in localized defects in the alveolar ridge: clinical results with different bone grafts and bone-substitute materials. *International Journal of Oral and Maxillofacial Implants* **24**(Suppl): 218–236.

Jovanovic, S.A., Schenk, R.K., Orsini, M. & Kenney, E.B. (1995) Supracrestal bone formation around dental implants: an experimental dog study. *International Journal of Oral and Maxillofacial Implants* **10**: 23–31.

Komori, T. (2006) Regulation of osteoblast differentiation by transcription factors. *Journal of Cellular Biochemistry* **99**: 1233–1239.

Lee, A., Brown, D. & Wang, H.L. (2009) Sandwich bone augmentation for predictable horizontal bone augmentation. *Implant Dentistry* **18**: 282–290.

Li, H., Jiang, J., Wu, Y. & Chen, S. (2012) Potential mechanisms of a periosteum patch as an effective and favourable approach to enhance tendon-bone

healing in the human body. *International Orthopaedics* **36**: 665–669.

Lian, J.B., Javed, A., Zaidi, S.K., Lengner, C., Montecino, M., van Wijnen, A.J., Stein, J.L. & Stein, G.S. (2004) Regulatory controls for osteoblast growth and differentiation: role of runx/cbfa/aml factors. *Critical Reviews in Eukaryotic Gene Expression* **14**: 1–41.

Lin, Z., Rios, H.F., Volk, S.L., Sugai, J.V., Jin, Q. & Giannobile, W.V. (2011) Gene expression dynamics during bone healing and osseointegration. *Journal of Periodontology* **82**: 1007–1017.

Linde, A., Thoren, C., Dahlin, C. & Sandberg, E. (1993) Creation of new bone by an osteopromotive membrane technique: an experimental study in rats. *Journal of Oral and Maxillofacial Surgery* **51**: 892–897.

Liu, Y. & Olsen, B.R. (2014) Distinct vegf functions during bone development and homeostasis. *Archivum Immunolgiae et Therapiae Experimentalis* **62**: 363–368.

McAllister, B.S. & Haghighat, K. (2007) Bone augmentation techniques. *Journal of Periodontology* **78**: 377–396.

Minkin, C. (1982) Bone acid phosphatase: tartrate-resistant acid phosphatase as a marker of osteoclast function. *Calcified Tissue International* **34**: 285–290.

Oh, T.J., Meraw, S.J., Lee, E.J., Giannobile, W.V. & Wang, H.L. (2003) Comparative analysis of collagen membranes for the treatment of implant dehiscence defects. *Clinical Oral Implants Research* **14**: 80–90.

Park, S.H., Lee, K.W., Oh, T.J., Misch, C.E., Shotwell, J. & Wang, H.L. (2008) Effect of absorbable membranes on sandwich bone augmentation. *Clinical Oral Implants Research* **19**: 32–41.

Park, S.H. & Wang, H.L. (2006) Management of localized buccal dehiscence defect with allografts and acellular dermal matrix. *The International Journal of Periodontics & Restorative Dentistry* **26**: 589–595.

Pietrokovski, J. & Massler, M. (1967) Alveolar ridge resorption following tooth extraction. *Journal of Prosthetic Dentistry* **17**: 21–27.

Pini Prato, G.P., Cairo, F., Tinti, C., Cortellini, P., Muzzi, L. & Mancini, E.A. (2004) Prevention of alveolar ridge deformities and reconstruction of lost anatomy: a review of surgical approaches. *The International Journal of Periodontics & Restorative Dentistry* **24**: 434–445.

Rothamel, D., Schwarz, F., Sager, M., Herten, M., Sculean, A. & Becker, J. (2005) Biodegradation of differently cross-linked collagen membranes: an experimental study in the rat. *Clinical Oral Implants Research* **16**: 369–378.

Schwarz, F., Rothamel, D., Herten, M., Sager, M. & Becker, J. (2006) Angiogenesis pattern of native and cross-linked collagen membranes: an immunohistochemical study in the rat. *Clinical Oral Implants Research* **17**: 403–409.

Schwarz, F., Rothamel, D., Herten, M., Wustefeld, M., Sager, M., Ferrari, D. & Becker, J. (2008) Immunohistochemical characterization of guided bone regeneration at a dehiscence-type defect using different barrier membranes: an experimental study in dogs. *Clinical Oral Implants Research* **19**: 402–415.

Siadat, H., Alikhasi, M., Mirfazaelian, A., Geramipanah, F. & Zaery, F. (2008) Patient satisfaction with implant-retained mandibular overdentures: a retrospective study. *Clinical Implant Dentistry and Related Research* **10**: 93–98.

Tatakis, D.N., Promsudthi, A. & Wikesjo, U.M. (1999) Devices for periodontal regeneration. *Periodontology* **2000**: 59–73.

Verdugo, F., D'Addona, A. & Ponton, J. (2012) Clinical, tomographic, and histological assessment of periosteal guided bone regeneration with cortical perforations in advanced human critical size defects. *Clinical Implant Dentistry and Related Research* **14**: 112–120.

Wang, H.L., Misch, C. & Neiva, R.F. (2004) "Sandwich" bone augmentation technique: rationale and report of pilot cases. *The International Journal of Periodontics & Restorative Dentistry* **24**: 232–245.

Wang, H.L. & Tsao, Y.P. (2007) Mineralized bone allograft-plug socket augmentation: rationale and technique. *Implant Dentistry* **16**: 33–41.

Supporting Information

Additional Supporting Information may be found in the online version of this article:

Appendix S1. CONSORT 2001 checklist.